

THE EFFECT OF NITROGEN CONTENT ON THE
SUSCEPTIBILITY TO STRESS-CORROSION CRACKING
OF TYPE 20Cr-20Ni AND AISI TYPE 310 STAINLESS STEELS

by

Ramaswamy Narayanan

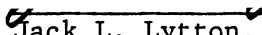
Thesis submitted to the Graduate Faculty of the
Virginia Polytechnic Institute and State University
in partial fulfillment of the requirements for the degree of

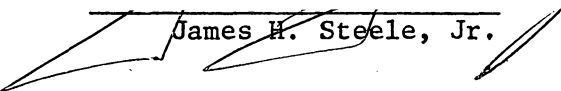
MASTER OF SCIENCE

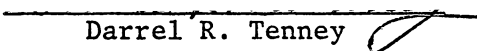
in

Metallurgical Engineering

APPROVED:


Jack L. Lytton, Chairman


James H. Steele, Jr.


Darrel R. Tenney

May, 1972

Blacksburg, Virginia

M

JCC 3-11-80

ACKNOWLEDGMENTS

The author would like to express his deep appreciation to Dr. Jack L. Lytton, Chairman of Metallurgical Engineering, Virginia Polytechnic Institute and State University, without whose guidance and encouragement the present investigation would not have been possible. In addition, appreciation is expressed to Dr. James H. Steele, Jr. and Dr. Darrel R. Tenney for their encouragement to the author during his study at this institution and for serving on the graduate committee.

The author sincerely appreciates the valuable assistance of Mr. Gary S. Clevinger throughout this investigation.

Appreciation is expressed to the United States Steel Corporation for supplying the stainless steel sheets used in this investigation, and to the United States Atomic Energy Commission for its financial support under contract No. AT-(40-1)-4052.

The author is indebted to his parents for their prayers and encouraging words and also to his brother Mr. R. Viswanathan, and to Mrs. Vatsala Viswanathan for their financial and moral support during his study in the United States. Last, but not the least, great appreciation is expressed to his wife for her immense patience and moral support during the author's scholastic endeavor.

TABLE OF CONTENTS

	<u>Page</u>
ACKNOWLEDGMENTS	ii
LIST OF FIGURES	iv
LIST OF TABLES	v
CHAPTER	
I INTRODUCTION	1
II REVIEW OF LITERATURE	4
III EXPERIMENTAL PROCEDURE	14
IV RESULTS AND DISCUSSION	20
Analytical Methods	20
Susceptibility of 20Cr-20Ni Alloy	22
Susceptibility of Type 310 Alloy	24
V CONCLUSIONS	32
VI RECOMMENDATIONS FOR FUTURE WORK	33
VII BIBLIOGRAPHY	52
VITA	55

LIST OF FIGURES

	<u>Page</u>
Figure 1. Apparatus used for stress-corrosion susceptibility test	34
Figure 2. Specimen holder	35
Figure 3. Schematic diagram of the gas nitriding system . . .	36
Figure 4. Schematic diagram of U-bend showing length and depth	37
Figure 5. Relationship between maximum crack length L and exposure time t, for various nitrogen levels in type 310 stainless steel	38
Figure 6. Relationship between maximum crack depth D and exposure time t, for various nitrogen levels in type 310 stainless steel	39
Figure 7a. Photomicrograph showing uniform nitrided case formed along the edges of a nitrided 20Cr-20Ni stainless steel specimen (0.161 wt.% N)	40
Figure 7b. As-homogenized microstructure of 20Cr-20Ni stainless steel containing 0.161 wt.% N	41
Figure 8a. As-nitrided microstructure of type 310 stainless steel containing 0.078 wt.% N	42
Figure 8b. As-homogenized microstructure of type 310 stainless steel containing 0.078 wt.% N	43
Figure 9. Scanning electron micrograph showing transgranular nature of stress-corrosion cracks in type 310 stainless steel containing 0.058 wt.% N tested for 18-1/2 hours in boiling magnesium chloride . . .	44
Figure 10. Example of a stress-corrosion crack observed in type 310 stainless steel U-bend specimens exposed for 18-1/2 hours in boiling magnesium chloride; right side is the specimen outer edge, and the left side is the convex face of the U-bend specimen	45

LIST OF TABLES

	<u>Page</u>
I Heat analysis of type 20Cr-20Ni stainless steel	46
II Heat analysis of type 310 stainless steel	47
III Nitriding atmospheres and resulting nitrogen contents	48
IV Solution annealing temperatures and times	49
V Relationship between exposure times and maximum crack depth for various nitrogen contents in type 310	50
VI Variation of rate of maximum crack propagation with penetration for various nitrogen contents in type 310 (using both L and D measurements)	51

I. INTRODUCTION

The problem of stress-corrosion cracking is one of the most serious problems in the development of reliable equipment in major industries. Stress corrosion may develop as fine intergranular or transgranular cracks with no evidence of corrosion products, and often there is no macroscopic evidence of the impending failure, (1).

Though stainless steels in general are considered to be resistant to corrosion, there are certain environments which render them susceptible to stress-corrosion cracking. Dixon (2) was the first to recognize this phenomenon in stainless steels. Since then stress-corrosion cracking in austenitic stainless steels has been recognized as a serious problem in chemical, petrochemical, and other related industries. Although much work has been done in this field, there is yet no single model of universal application which describes the initiation and propagation of stress-corrosion cracks.

Since nickel is a good austenite stabilizer and improves general corrosion properties in austenitic stainless steels, it has been suggested that by increasing nickel content, stress-corrosion cracking can be prevented. However, the addition of nickel proved to be costly. Considerable interest has been shown in the addition of nitrogen as an inexpensive means of increasing the strength and stability of the austenite phase. It was discovered in subsequent investigations, however, that increased nitrogen content in austenitic stainless steels promotes susceptibility to stress corrosion cracking, (3).

Early investigations at this institution were centered around a study of environmental variables affecting stress-corrosion cracking of U-bend specimens exposed to Mg Cl_2 solution boiling at 154°C . From these studies extensive evidence has been generated of aging effects in austenitic stainless steels at this temperature. Eckel and Manning (4) observed internal friction peaks in commercial AISI type 304 U-bend specimens, which they interpreted as being due to stress-induced diffusion of interstitial atoms (nitrogen and carbon) in the FCC lattice. A high purity 20Cr-20Ni alloy, also seemed to exhibit a similar stress-induced aging effect.

The results of other investigators on the susceptibility of high purity stainless steel containing 20Ni-(16-20)Cr in boiling 42% MgCl_2 have been conflicting. An alloy with 0.01N-0.01C has been shown by Barnartt and Van Rooyan (5) to be immune under severe testing conditions. Uhlig and White (6) found that an alloy containing 0.005N exhibited stress-corrosion cracking, while alloys having 0.001 and 0.002N were immune (0.01C each). Lang (7) reported variable results with an alloy containing 0.0001N and 0.001C, with cracks occurring in about 60% of the specimens. Further studies were needed to establish whether pure 20Cr-20Ni stainless steels are immune or susceptible and the role played by the presence of impurity elements.

The present investigation was undertaken to study and compare the effect of nitrogen on susceptibilities of a high purity 20Cr-20Ni alloy and commercial grade AISI type 310, each having nearly the same compositions in nickel and chromium but with significant differences

in other elements. A quantitative evaluation of the crack initiation and propagation rates of type 310 alloy has also been carried out for various nitrogen levels.

II. REVIEW OF LITERATURE

The present review considers stress-corrosion cracking of Fe-Ni-Cr alloys in aqueous environments. Extensive studies have been carried out to elucidate the nature of initiation and propagation of stress corrosion cracking in chloride solutions. There have also been numerous examples of cracking in caustic solutions (8,9).

Uhlig has defined stress corrosion cracking as the combined action of static stress and corrosion which leads to the spontaneous failure of the metal (10). It may be assumed from this definition that three conditions must be met for stress-corrosion cracking to be initiated:

1. susceptibility of the material to stress-corrosion cracking.
2. tensile stress on the surface of the material.
3. attack by specific corrosive agent.

Stress-corrosion cracking may be either transgranular or intergranular, depending upon the metal and corrosive medium. Since most of the observed cracking of austenitic stainless steels has been transgranular unless sensitized, the present discussion will be confined to the transgranular mode.

Transgranular stress-corrosion cracking in austenitic stainless steels is considered to be a two-stage phenomenon, consisting of an induction time during which cracks are initiated, and a propagation time during which they propagate to failure. Harwood (11) in

discussing a paper by Uhlig suggested that stress corrosion is a two-stage process consisting of crack initiation and propagation. Two stages were also suggested by Forty (12) to explain stress-corrosion cracking in alpha brass and similar alloys. Logan (13) has shown abrupt changes in deflection rates of an uniaxially loaded stainless steel specimen which he interpreted as the start of crack propagation after periods of incubation. Hoar and Hines (14) studied time-potential curves obtained with stressed wire exposed to boiling $MgCl_2$ and they suggested that the incubation period consisted of an attack on the protective film. Clevinger and Lytton (15), however, have found very fine cracks during the apparent "incubation period" in type 304 U-bend specimens using scanning electron microscopy techniques.

When an attempt is made to propose a useful theory of stress-corrosion cracking, one should be able to explain at least the role of the following:

1. percentage of major alloying elements
2. impurity content
3. corrosive environment
4. magnitude of stress
5. temperature of test
6. initiation and propagation stages in producing failure.

All theories proposed may be categorized into two broad groups. According to one group, stress-corrosion cracking is purely an

electrochemical phenomenon and it propagates in a direction normal to the tensile stress. According to this mechanism, a definite period of time is required for a crack to initiate, after which it grows at a rate controlled by the anodic metal dissolution reaction at the advancing tip of the crack.

The mechanism favored by the second group is a periodic mechanism in which the corrosive action proceeds for some time until it triggers a short mechanical fracture. The mechanism of rapid mechanical fracture was proposed by Keating (16). According to Keating, the mechanical fracture step is initiated when a stress-concentrating notch is located at an appropriate lattice site or boundary. But Nielson (17) concluded from electron microscopic studies of stress corrosion products deposited within the cracks that the solid corrosion products can exert a wedging action and produce a periodic mechanical fracture.

The various theories proposed indicate that on one hand the physical aspects such as microstructure, film rupture, or solute segregation play a dominant role while on the other hand, the electrochemical aspects such as dissolution kinetics or anion diffusion may play an important role.

Considerable attention has been given in the literature to the importance of alloying elements on the susceptibility of austenitic stainless steels to stress-corrosion cracking. For example, extensive studies have been conducted on the influence of molybdenum.

Barnartt, et al (18), have proved that the addition of 1.5% Mo to an originally immune Fe-20Ni-16Cr alloy, renders it susceptible to stress-corrosion cracking. Van Rooyan (19) found that the effect of molybdenum is significantly detrimental at about 0.1%-0.2% in a 20% Ni alloy. Truman and Perry (20) investigated the effect of molybdenum additions to Fe-(15,25,35)Ni-15Cr alloys and found no significant effects up to 2.5%-5% additions of molybdenum. It is clear from the available information that molybdenum additions appear detrimental in the 0.1% to 0.4% range when added to 8% Ni and 20% Ni base alloys.

Ohtani and Dodd (21) observed the detrimental effect of molybdenum in a 20Cr-20Ni alloy. They suggested that the addition of molybdenum probably reduces the stacking fault energy in this type of steel leading to the following mechanism: deformed steel of low stacking fault energy (due to the addition of molybdenum) contains coplanar groupings of extended dislocations, so that at the susceptibility testing temperature sigma platelets may form along active slip planes. This accentuates both local galvanic corrosion and brittle mechanical cracking.

Lang (7) has studied the effect of phosphorus in the range 0.065%-0.350% on austenitic stainless steels of type 20Cr-20Ni. She observed that the resistance of this alloy to transgranular cracking is lowered by the addition of 0.30% P. Swann (22), using transmission electron microscopy, pointed out the harmful effect of 0.35% P in a 20Cr-20Ni alloy in terms of dislocation structures. Thomas, et al. (23), have shown that by the addition of 0.3% P to a 20Cr-20Ni base

alloy, the degree of short range order is increased and slip is restricted to well-separated planes, giving rise to planar arrangements and making the material susceptible to stress-corrosion cracking. Recently, Masamichi and Fujikawa (24) have studied the combined effect of phosphorous and nitrogen on an 18Cr-10Ni alloy. They concluded that stainless steel containing less than 0.003% P did not exhibit stress-corrosion cracking in boiling $MgCl_2$ solution even with nitrogen contents up to 0.08%.

The effect of higher nickel contents in promoting resistance to stress corrosion cracking is well known. Copson (3) demonstrated the effect of nickel in delaying cracking time. Robertson and Tetelman (25) rationalized this in terms of an increase in stacking fault energy with increasing nickel content. Though the effect of nickel has thus been explained, the effect of interstitial atoms like carbon, nitrogen and phosphorus has been under extensive study; to date, none of the theories suggested seems satisfactory.

The effect of nitrogen in increasing the susceptibility of austenitic stainless steels to stress-corrosion cracking was first reported by Uhlig, et al. (26), and later confirmed by others (27, 28, 29, 30, 31). Uhlig, et al., suggested that the precipitation of a finely divided second phase, in which carbon or nitrogen participate, directly or indirectly increases the corrosive attack, thereby rendering the metal more susceptible. Uhlig and White (6) compared several commercial alloys with those prepared in their laboratory. They observed that commercial alloys of 25Cr-20Ni cracked in shorter times than any of the alloys prepared in the laboratory, indicating that

elements in addition to nitrogen participate in the cracking mechanism. They concluded that in a pure 20Cr-20Ni alloy, the cracking of the stable gamma austenitic phase is associated mainly with nitrogen content. Although this explanation may be valid for the effect of nickel, Uhlig and Sava (27) also observed an aging effect in type 310 stainless steels, which they concluded to be the result of segregation of nitrogen atoms to dislocations and precipitation of nitrides from austenite supersaturated with nitrogen at 154°C.

Lang (7) studied the effect of individual element additions to a 20Ni base alloy and concluded that if alloys were sufficiently pure, they would be resistant to cracking in long-time tests.

Barnartt and Van Rooyan (5) observed vigorous evolution of hydrogen from stress-corrosion cracks in austenitic alloys containing nitrogen and no such effect from alloys with little or no nitrogen. In addition, the evolution of hydrogen was observed at pH values and potentials where thermodynamic considerations predict no hydrogen gas formation. It was concluded that nitrogen or some other second phase containing nitrogen acts catalytically, effecting an increase in the cathodic reduction of hydrogen ion, thereby increasing the corrosion current.

Both Ferry (28), and Eckel and Manning (4), from their experiments on dilatometric and internal friction measurements, have shown sufficient evidence for a precipitation phenomenon occurring in these alloys around the stress-corrosion testing temperature (154 °C).

Cox (29) has also shown that aging at 154°C of various commercial austenitic stainless steels containing various levels of nitrogen in solid solution, increases the susceptibility in these alloys.

There is also considerable evidence in the literature which indicates that the dislocation substructure may play an important role in determining the stress-corrosion susceptibility of various alloys. It has been observed that alloys with a cellular arrangement of dislocation tangles exhibit superior resistance to transgranular stress-corrosion cracking compared to those containing planar group of dislocations. This means that in alloys having low stacking fault energy in which there is limited cross slip, the dislocations tend to form coplanar arrays which are more detrimental to the resistance of the alloy.

The important role of stacking fault energy on stress corrosion susceptibility was first suggested by Forty (12). Robertson and Tetelman (25) expanded this idea to propose a unified theory for both transgranular and intergranular failure. They postulated that a high degree of dislocation coplanarity due to low stacking fault energy increases the susceptibility to cracking. They also observed that low stacking fault energy in these alloys stabilized Cottrell-Lomer barriers. This is in agreement with the earlier observation of Robertson and Bakish (30) that dislocation pileups at these Cottrell-Lomer barriers are sites for preferential dissolution of metals, producing crack-sensitive paths.

Swann (22) attempted to account for the apparently opposite

effects of carbon and nitrogen on the susceptibility in terms of different substructures present in the plastically deformed alloys. Austenitic stainless steels containing nitrogen in excess of nominal amounts were found to deform by coplanar glide of dislocations, while a cellular substructure resulted from the presence of carbon. Swann studied the microstructure of deformed alloys which are susceptible to stress-corrosion cracking by transmission electron microscopy and found a strong relation between the distribution of dislocations and the susceptibility of the alloys to stress-corrosion cracking. In his investigation, the stacking fault energy was varied by the addition of nickel and nitrogen and he found that susceptible alloys exhibited a greater frequency of coplanar dislocation configurations.

Various opinions have been expressed concerning the reason why a coplanar mode of dislocation glide should correlate with an increased susceptibility to transgranular cracking. Among other things, they include a preferential electrochemical attack along a continuous plane of disordered material in a short-range ordered matrix; possibly resulting from segregation of solute atoms to the coplanar groups of dislocations, and the easier rupture of protective surface films by the larger slip steps associated with coplanar glide.

Douglas, et al. (31), Thomas, et al. (23), and Swann and Nutting (32) associated coplanarity of dislocations to short-range order in a susceptible alloy. As a result of short-range order the apparent stacking fault energy of a system may be increased but dislocations

move as coplanar groups, initially in pairs, so that dislocation substructures are qualitatively similar to those found in metals of low stacking fault energy. Although short range order decreases the equilibrium separation of partials, cross slip will be blocked as a result of ordering (31). Thus transgranular stress-corrosion cracking can occur in alloys of high stacking fault energy if strong local order exists.

It has been shown by various investigators (27,28,29,30,31) that nitrogen appears to have a detrimental effect on stress corrosion cracking. Short-range ordering and other structural considerations cannot be solely responsible for the observed decrease in resistance. It is more likely that a combination of structural properties and enhanced localized electro-chemical activities are responsible for the general effect of nitrogen in these alloys.

Honeycomb, et al. (33), observed that stacking fault energy is decreased considerably by the presence of carbide- and nitride-forming elements. Douglas, et al. (31), observed that dislocations are arranged in coplanar groups in a 20Cr-20Ni alloy in the presence of nitrogen, even though stacking fault energy measurements indicate that these alloys should exhibit extensive cross-slip and therefore tangled dislocation configurations.

Smith (34) and Clevinger (35) at this institution, have shown that dislocation configurations in 20Cr-20Ni alloys are related to both nitrogen content and to strain level, a higher pre-strain being

required to produce tangling in alloys having increased nitrogen contents.

Maitra (36) has shown that nitrogen increases the susceptibility of AISI type 304 wires to stress-corrosion cracking. His data indicates that for a known stress level, increased nitrogen content results in decreased times to failure. Maitra further concluded that the effect of nitrogen in these alloys is largely electrochemical, based upon the observation that increased nitrogen content caused a significant decrease in failure times at stresses below the yield point for this material, where mechanical effects would be minimized.

III. EXPERIMENTAL PROCEDURE

The as-received materials for this investigation were supplied by United States Steel Corporation in the form of rolled sheet approximately 1/16" thick with a 2B finish. The chemical analysis of the two materials, as provided by the supplier, are recorded in Tables I and II. It is important to note the very low level of impurity content in the 20Cr-20Ni alloy. The nitrogen contents of the as-received 20Cr-20Ni and type 310 alloys were determined by the author to be 0.004 wt.% and 0.033 wt.% respectively.

The specimens were cut from the as-received sheets with the longest dimension transverse to the rolling direction and milled to the final dimensions of 1/2" by 5". Holes 3/16" in diameter were drilled on center, 1/2" from both ends of the specimen.

The specimens were then polished carefully using 240,320 and 600 grit CarbiMet polishing papers, washing thoroughly between steps with water. The direction of polishing was such that the scratches were always parallel to the longest dimension of the specimens. This was to avoid producing scratches in the expected growth direction of cracks. Polished specimens were finally washed with methanol to ensure the removal of all possible surface contaminants. Nitrogen was then introduced into the specimens.

The nitriding system used in this investigation is a modified form of the one used by Eckel and Cox (37). The schematic diagram of the nitriding system is shown in Figure 3. It consists of three

separate gas trains, one each for nitrogen, hydrogen, and ammonia. Valving is provided so that these could be used either individually or in combination. Each of these gas trains has a suitable chemical reagent to remove the oxygen and moisture from the commercial gas used. In order to remove the moisture content, the gases are passed through two drying furnaces, one containing palladized alumina at 400°F and the other containing copper wire maintained at 250°F. The reaction chamber consists of a tubular furnace 61cm long, which surrounds a glazed mullite tube with an inside diameter of 2.8cm. By proper shunting, a uniform heating zone 28cm long is maintained in the furnace.

In each run, four specimen blanks were placed inside the furnace with ceramic pellets separating them to avoid specimen-to-specimen contact. The nitriding system was properly sealed to avoid air leaking into the system and producing surface oxides on the specimens. After sealing, the entire system was purged for about 45 minutes in the specified atmosphere. The total flow of the gases was adjusted to the desired level, and was calibrated by using a graduated burette which served as the flow-meter. The gases were bubbled through a soap solution contained in a bulb fitted to the bottom of the burette and the rate of gas flow through the system was measured from the time taken by a bubble to traverse a given length of the burette. After the purging period, the furnace power was turned on and the reaction chamber was held at the required temperature for the desired time. The power was then turned off and the specimens were allowed

to cool to room temperature inside the furnace while the gas flow was maintained. The combination of gas mixtures used in the present investigation and the various nitrogen levels obtained are listed in Table III.

In order to obtain a uniform distribution of nitrogen in solid solution in the nitrided specimens and to avoid precipitation of nitrides, a homogenization treatment was necessary. This was achieved by encapsulating the specimens individually in evacuated Vycor tubing followed by a diffusion annealing treatment, after which they were quenched in water by breaking the tube. After the solution annealing treatment, it was necessary to pickle the specimens to remove the oxide layer formed during quenching. Long pickling time was avoided to prevent excessive pitting. Pickling was carried out in two successive steps, first using a bath of 10% H_2SO_4 followed by another of 10% HNO_3 - 2% HF. In practice it was found that bath temperatures of 60 °C resulted in effective pickling of the oxide layer with a minimum of surface pitting.

When 20Cr-20Ni stainless steel specimens were nitrided in an atmosphere of $60NH_3$ - $40H_2$ at a flow rate of 400CC/minute at 1800 °F, a heavy, uniform nitride case was formed on the surfaces of the specimens, as shown in Figure 7a. It was found that a homogenization annealing treatment of 2300 °F for 30 minutes gave a fully homogenized structure, as seen in Figure 7b. Figure 8a is a photomicrograph of a type 310 specimen in the nitrided condition (0.078 wt.% N) showing the nitrided precipitates distributed along the grain boundaries.

Figure 8b shows the structure of the same specimen in the homogenized condition, with nitrogen in solid solution.

A standard volumetric technique known as the modified Kjeldahl method was followed for determining nitrogen contents in as-received and nitrided samples. The procedure was supplied by Allegheny Ludlum Steel Corporation. The procedure required that samples weighing approximately 0.5 grams be dissolved in 70% perchloric acid to which an excess of caustic is added to evolve ammonia. The ammonia thus formed from the nitrogen in the sample is steam distilled into a boric acid solution containing an indicator mixture of bromocresol green and methyl red and titrated against standardized sulfuric acid solution to end point.

Following the solution annealing treatment, the as-received and the nitrided samples were bent into the U-bend shape by mechanically forcing them around a one-inch diameter mandrel. Stainless steel bolts of 18Cr - 8Ni composition were inserted through the drilled holes and tightened with nuts until the inside dimension at the bolts was 1". This ensured an inner diameter of one inch at the curved section of the specimen. Teflon washers were used to prevent metal-to-metal contact between the bolt and the U-bend specimens. Prior to the exposure in magnesium chloride, the specimens were allowed to sit in the laboratory atmosphere for 24 hours so that a uniform passive film could be formed on the surface.

The stress-corrosion test apparatus used in this investigation was similar to that designed by Streicher and Sweet (38) and is shown

in Figure 1. It consisted of a 1000ml Huey corrosion flask fitted with a reflux condenser. The flask contained a thermometer well in which mercury was placed for quick response to the temperature of the solution contained in the flask. A mercury-in-glass thermometer was placed in the well to read the temperature of the solution directly.

In order to avoid inconsistency of the results during long-time exposure tests due to variations in testing environment, the following modifications were incorporated:

1. A vapor trap was provided at the top of the condenser column to avoid vapor losses from the boiling magnesium chloride.
2. Evaporation of condensate from the top of the ground-glass joint was essentially eliminated by wrapping the joint with commercial aluminum foil.
3. The condenser with cool-joint was redesigned, so as to effectively direct the condensate to the walls of the flask as a liquid film.

Solutions of 42% $MgCl_2$ were prepared by mixing 550 grams of technical grade magnesium chloride flakes with 15ml of distilled water in the Huey flask. The contents were heated to boiling. If the temperature of the solution was more than $154^{\circ}C$ distilled water was added and if the temperature was below $154^{\circ}C$ it was allowed to boil in an open flask momentarily. All the U-bend specimens were then tested for susceptibility by exposing them individually in freshly prepared magnesium chloride boiling at $154^{\circ}C$. In order to avoid contact between the

U-bend specimens and the bottom of the flask, a special holder was designed and constructed, and is shown in Figure 2. The time of exposure was calculated from the time of immersion to the time of removal.

Specimens were washed thoroughly with distilled water after removal from the magnesium chloride solution and then dried. Cracks were viewed along the convex surface of the specimens at 110X under a bench microscope using a calibrated eyepiece. Crack depths were measured in terms of number of divisions of the eyepiece and converted to microns by a suitable calibration factor.

Samples were prepared for scanning electron microscopic study by suitably cutting the U-bend specimen, so that the bent portion could be mounted on a platform designed for this purpose. Observations were made along the convex surface of the U-bend using secondary electrons. Typical cracks observed by scanning electron microscope are shown in Figures 9 and 10.

IV. RESULTS AND DISCUSSION

Analytical Methods

The relative susceptibilities to stress-corrosion cracking of the specimens used in this investigation were determined using the general analytical methods developed by Eckel (39). In those studies, measurements of depth of longest crack in stainless steel U-bend specimens as a function of exposure time in boiling magnesium chloride at 154°C suggested that a plot of maximum crack depth as a function of logarithm of exposure time produces a straight line. This results in an analytical expression of the form:

$$\log_{10} t = D/M + \log_{10} t_0 \quad (1)$$

where, t = total exposure time

D = maximum crack depth

M = slope of the plot D versus $\log_{10} t$

and t_0 = the "initiation time"

Analysis of this equation shows that the rate of growth of the longest crack can be obtained directly by differentiating Equation (1) with respect to time. The resulting equation is:

$$\frac{dD}{dt} = \frac{0.4343M}{t} \quad (2)$$

It should be pointed out that Equation (2) produces an infinite crack propagation rate at $t=0$, a point at which it has been presumed

that no cracks have been formed. It therefore appears that Equation (1) is not physically adequate to represent a time law for stress-corrosion cracking. Clevinger and Lytton (15) utilizing the data of Eckel have developed and examined an alternate equation which has improved physical interpretation. The equation is of the form:

$$D = D_m [1 - \exp(-t/\tau_{Sc})] \quad (3)$$

where, D = crack depth

D_m = maximum possible crack depth

t = exposure time

and τ_{Sc} = a stress-corrosion time constant.

This equation produces the following formulation for the rate of propagation:

$$\frac{dD}{dt} = \frac{D_m}{\tau_{Sc}} \exp(-t/\tau_{Sc}) \quad (4)$$

which predicts that, as expected for U-bend specimens, crack propagation rate would decrease with exposure time. It also indicates that crack propagation rate at $t=0$ is equal to $\frac{D_m}{\tau_{Sc}}$ rather than infinity. The use of Equation (3) to represent U-bend crack depth data produces the following characteristics:

1. Crack depth cannot be greater than the specimen thickness.
2. Crack propagation rate decreases with time.
3. Complete penetration through the specimen thickness will not be obtained in finite time.

4. Crack propagation will begin immediately upon exposure.

The determination of the dimensions of the most severe cracks was in fact accomplished by two distinct methods in this investigation. The first method, after Eckel, was to measure by optical microscopy the depth in microns of the longest crack on the edge of the specimen, beginning at the outer fibers of the convex face and traversing along a radius of the U-bend configuration. This measurement is referred to as D in the analytical expressions, and is identified schematically in Figure 4. A second method of measuring the extent of cracking was devised for this investigation, and required the measurement of the length in microns of the longest crack on the convex face of the U-bend specimen. This measurement is denoted as L in Figure 4.

The data collected in this investigation were analysed using both the standard equation developed by Eckel and new equation developed by Clevinger and Lytton.

Susceptibility of 20Cr-20Ni Alloy

The tendency for increased nitrogen content to increase the susceptibility of austenitic stainless steels to stress-corrosion cracking has been described in detail in the literature review. In order to isolate the effects of nitrogen content on the susceptibility of these alloys, a series of tests were designed using a highly pure austenitic alloy containing 20% Chromium and 20% Nickel with very low impurity contents. This alloy contained 0.004 wt.% nitrogen in solid solution and was recognized to be highly resistant to stress-corrosion

cracking. U-bend specimens were prepared from the as-received material using the procedure outlined previously, and these were subsequently exposed to MgCl_2 boiling at 154°C . Examination of these specimens after exposure revealed, however, that the as-received material was even more resistant to cracking than was previously thought. Various exposure times up to 356 hours produced no evidence of stress-corrosion damage in these specimens. Table V gives a detailed listing of the exposure times studied.

The experiment at this stage still offered promise, however, provided the resistance of the material could be substantially reduced by nitrogen additions in solid solution. Accordingly, samples were nitrided and homogenized to yield a composition having 0.161 wt.% nitrogen in solid solution. Again, U-bend specimens were fashioned and exposed for as long as 260 hours in MgCl_2 boiling at 154°C . As before, examination revealed that no stress-corrosion cracking had occurred in these specimens even with the much higher nitrogen contents.

The continued resistance of type 20Cr-20Ni austenitic stainless steel to stress-corrosion cracking even after significant nitrogen additions is perhaps an indication that the observed effect of nitrogen additions on alloys having commercial purity is inter-related with other compositional variables. Recent work by Kowaka and Fujikawa (24) also supports this premise. These authors have suggested that a minimum amount of phosphorus is required in austenitic alloys in order for nitrogen additions to be effective in increasing susceptibility. They have shown that an 18Cr-10Ni alloy containing less than 0.003%

phosphorus does not cause stress-corrosion cracking even at high nitrogen levels of 0.08%. However, the detrimental effect of nitrogen, according to them, appeared when the phosphorus content was increased to more than 0.003%.

Susceptibility of Type 310 Alloy

The extremely high resistance of the 20Cr-20Ni alloy to stress-corrosion cracking effectively prohibited the determination of the effect of nitrogen additions on the susceptibility. An alternative investigation was undertaken using commercially available type 310 austenitic stainless steel, which has approximately the same content of major alloying elements but considerably higher impurity content than the 20Cr-20Ni alloy. The type 310 alloy also has good cracking resistance, but exhibits stress-corrosion failure after several hours of exposure in $MgCl_2$. U-bend specimens of type 310 having the as-received composition were prepared and tested in $MgCl_2$ boiling at $154^\circ C$. Stress-corrosion cracks were observed after exposure and the dimensions of the longest cracks in both the edge and the convex surface were recorded. Subsequent samples having higher nitrogen contents (0.058 wt.% and 0.078 wt.% respectively) were given various exposure times and examined in the same fashion. Table V presents a detailed tabulation of these data. As expected, the data indicate that longer exposure times induce longer and deeper cracks in the specimens. There is also good indication that increased nitrogen content produces more severe cracking for a given exposure time, particularly for the L values

which were measured on the convex surface of the U-bend specimen. A plot of crack length, L , versus log exposure time for the three nitrogen levels using the equation developed by Eckel is shown in Figure 5. The effect of increase in nitrogen content is immediately apparent, i.e. increasing nitrogen contents result in decreasing the crack initiation times. The crack initiation time for the material containing 0.033 wt.% nitrogen is 8.5 hours; increasing the nitrogen levels to 0.058 wt.% and 0.078 wt.% results in decreases in the crack initiation times of 6.5 hours and 3 hours respectively. It is also clear from the Figure that increasing nitrogen content increases the depth of penetration for a given exposure time. However, the increase in nitrogen content does not seem to influence appreciably the slope M of the straight lines drawn at various nitrogen levels. The dashed lines indicate the relationship predicted by the equation developed by Clevinger and Lytton for the same data. The two equations coincide very well except for very short exposure times, where the exponential equation predicts that small cracks would be predicted during the induction period predicted by Equation (1).

A plot of maximum crack depth, D , versus exposure time is shown in Figure 6 for the three nitrogen levels. The correlations are poor for these data, possibly because only one specimen was examined for each exposure time. In the studies performed by Eckel and Cox (37) on type 304 stainless steel, average crack depth for several specimens were used to produce correlations. The use of single specimens appear to have increased the experimental scatter and therefore does not

clearly define the effect of nitrogen. It is significant to note also that the use of equation (1) with measurements of L predicts an incubation period of 8.5 hours for 0.033 wt.%N while the same equation predicts an incubation time of less than 6 hours for the same material using measurements of maximum crack depth D.

The rates of maximum crack propagation were calculated for each alloy at various percentages of penetration. These rates were calculated using both Equation (2) and Equation (4) and utilizing both L and D measurements. These data are presented in Table VI. The propagation rates calculated from L measurements indicates that the rate of growth of the cracks increases with increasing nitrogen content and that the growth rate decreases as the cracks continue to propagate. This trend is consistent for rates calculated with either Equation (2) or Equation (4).

The cracked specimens of type 310 were examined by scanning electron microscopy with particular attention being given to the configuration and location of the cracks. The high depth of field in scanning electron microscopy allowed the cracks to be observed as it passed around the corner of the specimens. Some of the long cracks had "hair line" extensions at their tips which could not be resolved by the bench microscope. These were, however, resolved by scanning electron microscope. These were, however, resolved by scanning electron microscope at high magnification. It was observed that the cracks were transgranular and extensively branched, and were generally located near the edges of the convex surface within 50 degrees on either side of the U-bend tip. In specimens having longer exposures, however,

localized groupings containing a large number of cracks were observed which traversed the entire width of the convex face. This was in contrast to the random distribution of cracks seen in specimens having shorter exposure times. Photomicrographs of typical cracks observed in type 310 alloy by scanning electron microscopy are shown in Figures 9 and 10. Figure 9 shows the transgranular nature of the crack. Corrosion products can be seen along the length of these cracks. An example of the branching nature of the crack is shown in Figure 10. The branching crack is on the left. The specimen outer edge is at the right and the convex face of the U-bend specimen is at the left.

The observed differences in the stress-corrosion susceptibility between type 310 and 20Cr-20Ni stainless steel can apparently be attributed solely to the relative purity of the two alloys. The commercial grade type 310 contains much higher levels of impurity additions than does the laboratory grade 20Cr-20Ni material, which is basically a high purity alloy. There are various tentative explanations for the effect of these impurity elements on the susceptibility. Lang (7) reported the effect of phosphorus in increasing the susceptibility to stress-corrosion cracking in alloys containing about 21% nickel and 18.5% chromium. She showed that an increase in phosphorus content from 0.003% to 0.065% reduced the average cracking period of these alloys from 23 days to one day. Kowaka and Fujikawa (24), for example, have asserted that the combined effect of phosphorus and nitrogen is important in increasing the susceptibility in an alloy containing 18% chromium and 10% nickel. They found that minimum levels

of phosphorus are required in order for increases in nitrogen to increase the susceptibility of certain grades of stainless steels. The phosphorus content in type 20Cr-20Ni alloy is significantly lower than in type 310. It is possible that in type 20Cr-20Ni alloy the effect of nickel content in increasing the resistance to stress-corrosion cracking more than compensates for the combined effect of phosphorus and nitrogen in increasing the susceptibility. In type 310, however, the increased levels of phosphorus and nitrogen may overbalance the beneficial effects of nickel and lead to enhanced susceptibility. It would be interesting to observe the effect of higher phosphorus contents in conjunction with increased nitrogen levels on the susceptibility of type 20Cr-20Ni austenitic stainless steels.

Investigators (40,41) of a proposed electrochemical mechanism of stress-corrosion cracking have discussed the role of anodic reactions at susceptible paths in the material, but the cathodic part of the corrosion reaction, i.e. hydrogen evolution and absorption by austenite, has been dispatched by most workers (42,43), because the amount of hydrogen absorbed by the steel during corrosion is small. The presence of even a small amount of elements such as phosphorus, sulphur and arsenic polarize or "poison" the hydrogen evolution reaction. These poisons could inhibit the recombination of hydrogen atoms on a surface and thereby increase the availability of hydrogen for penetration of the substrate.

A mechanism for the formation of susceptible paths based upon the reaction and diffusion of hydrogen would partially explain differences

in susceptibility of type 310 and 20Cr-20Ni stainless steels to stress-corrosion cracking in terms of their compositional variations and the effect of increases in nitrogen content.

Logan and Sherman (44) have observed hydrogen gas escaping from stress corrosion cracks in stainless steels. It was shown by Vaughan, et al. (45) that hydrogen when in solid solution diffuses through the austenite lattice under applied stress and forms a stress oriented transgranular hydride precipitate phase distribution in the path of the crack. This type of orientation was observed to be in a direction normal to the tensile direction. Hydrogen seems to react with the austenitic stainless steels and under an applied load forms a phase which is distributed so as to resemble the susceptible path followed by stress corrosion cracks. As the hydride reacts with magnesium chloride, gas bubbles are evolved rapidly. The hydrogen thus released from the hydride phases may react with the metal at the bottom of the crack to further elongate the susceptible path. This precipitate phase distribution may be totally absent in type 20Cr-20Ni alloy because of insufficient impurities for this precipitate reaction to occur. Even an increase in nitrogen level in this alloy did not have any effect on the susceptibility. This clearly indicates that besides nitrogen, other impurities like carbon and phosphorus are necessary in this alloy in order to induce susceptibility.

Uhlig and Sava (27) observed an aging effect on type 310 stainless steels which is probably caused mostly by segregation of nitrogen atoms at dislocations and by precipitation of nitrides from austenite

supersaturated with nitrogen at 154°C. They suggested that the precipitation of a finely divided second phase, in which carbon or nitrogen participate directly or indirectly, increases the corrosive attack, thereby rendering the material more susceptible. Clevinger (35) observed small precipitates in type 20Cr-20Ni nucleating on slip planes after relatively short aging times at 154°C. In this investigation, unaged samples of this material with very high nitrogen contents were found to be immune even after 260 hours of exposure in $MgCl_2$ boiling at 154°C. It would be interesting to determine whether extensive aging with high nitrogen contents would in fact induce stress-corrosion cracking.

An additional factor to consider is that increases in interstitial solute content lead to an increase in the flow stress in the material (34). If it were true that the increase in nitrogen content is principally to strengthen the alloy, then for a given stress level, the susceptibility would be expected to decrease with increasing nitrogen content. Furthermore, the U-bend test used produces constant surface strains and therefore increased stresses with increasing nitrogen content. Consequently, it is not possible to clearly differentiate between the mechanical and electrochemical effects of nitrogen additions using the U-bend test. Using known tensile stresses applied to wires exposed to boiling $MgCl_2$, however, Maitra (36) has concluded that the effect of nitrogen in type 304 stainless steel is largely electrochemical. This was based upon the observation that increased nitrogen content caused significant decrease in failure times at stress levels well below the yield point, where mechanical effects were minimized.

It is therefore suggested that the observed increase in susceptibility in type 310 with increasing nitrogen content represents predominantly an electrochemical phenomenon.

V. CONCLUSIONS

1. Type 20Cr-20Ni austenitic stainless steel containing 0.004 wt.% nitrogen did not crack even after 356 hours of exposure in boiling MgCl_2 .
2. No stress-corrosion cracking occurred in type 20Cr-20Ni stainless steel specimens even at 0.161 wt.% nitrogen.
3. Type 310 austenitic stainless steel containing 0.033 wt.% nitrogen exhibited susceptibility to stress-corrosion cracking in boiling MgCl_2 with an apparent incubation period of 8.5 hours.
4. Increase in nitrogen content from 0.033 wt.% to 0.078 wt.% decreased the crack incubation time from 8.5 hours to 5.0 hours in type 310 stainless steel.
5. The depth of penetration increased with increasing nitrogen content for a given exposure time in boiling MgCl_2 for type 310 stainless steel specimens.
6. The rate of propagation of stress-corrosion cracks in U-bend specimens of type 310 decreased with increasing depth of penetration.
7. It is suggested that differences in stress-corrosion susceptibility between type 310 and 20Cr-20Ni are related to differences in their phosphorus and nitrogen contents.
8. It is suggested that the observed increase in susceptibility in type 310 with increasing nitrogen content represents a predominantly electrochemical phenomenon.

VI. RECOMMENDATIONS FOR FUTURE WORK

In the light of the present investigation, the following recommendations are made for future work:

1. It would be interesting to study the stress-corrosion susceptibility in type 20Cr-20Ni alloy by increasing its phosphorus content and study the combined effect of phosphorus and nitrogen.
2. It is recommended that an investigation should be directed towards the effects of precipitation of nitrides by aging a high nitrogen, 20Cr-20Ni alloy for very long times and study the aging effects of nitrogen on the stress-corrosion susceptibility of this material.
3. Crack initiation times should be studied by scanning electron microscopy and it is also recommended that an intensive x-ray analysis of the corrosion products present along the susceptible path should be carried out.

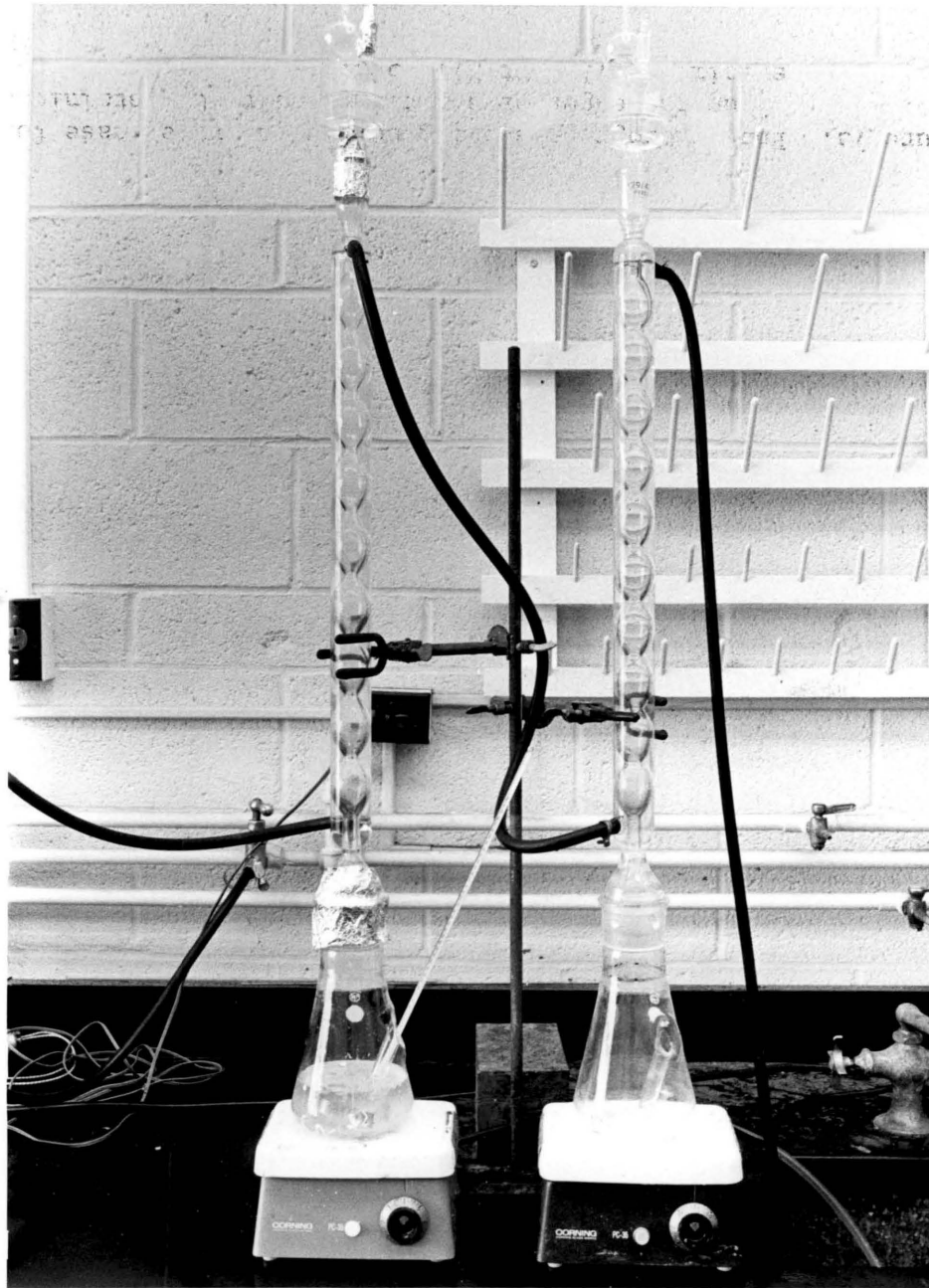


Figure 1. Apparatus used for stress-corrosion susceptibility test.

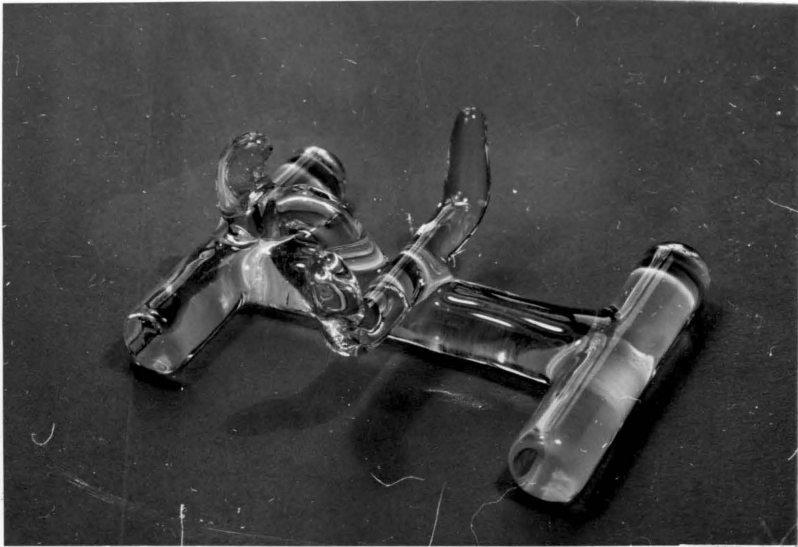


Figure 2. Specimen holder.

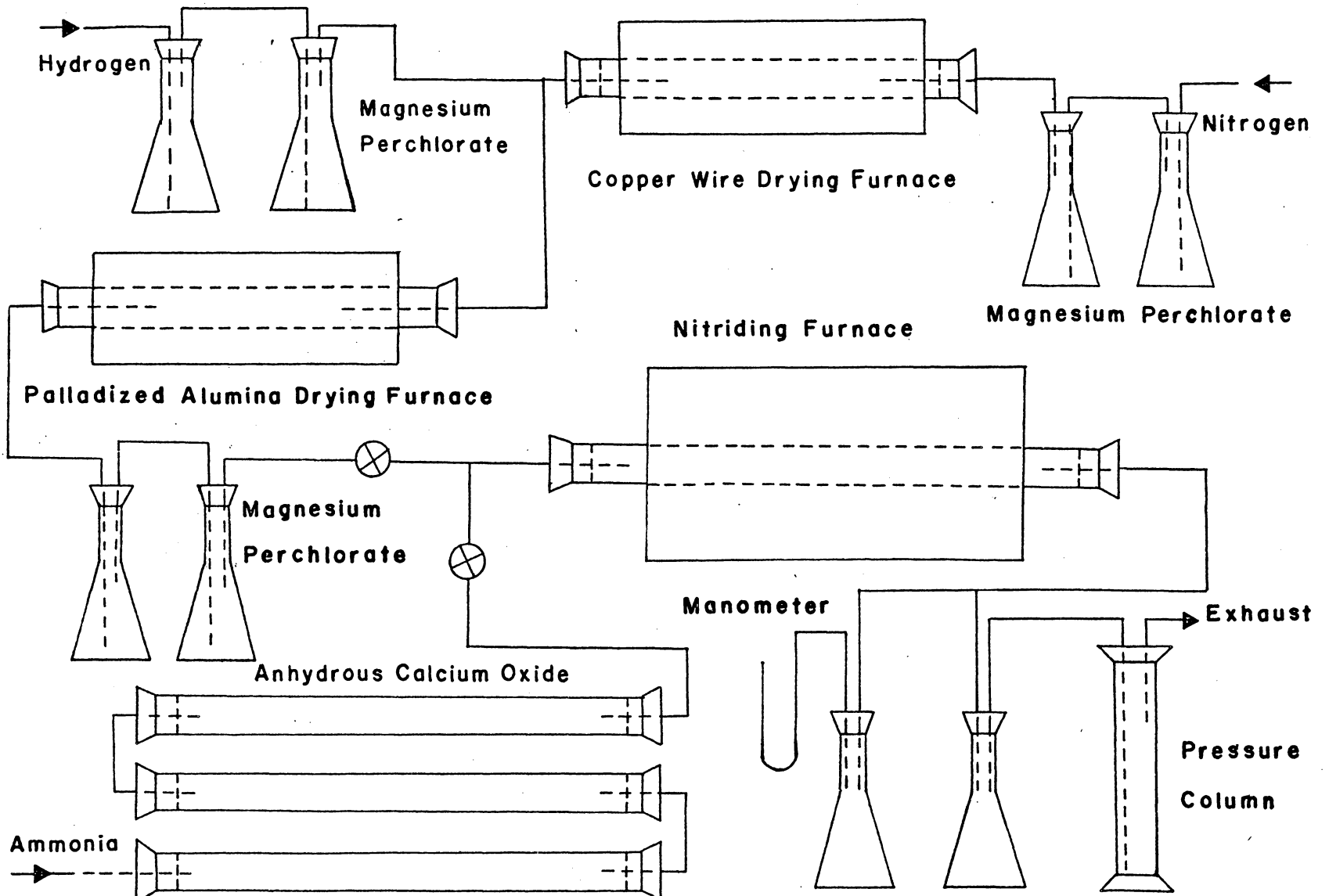


Figure 3. Schematic Diagram of the Gas Nitriding System.

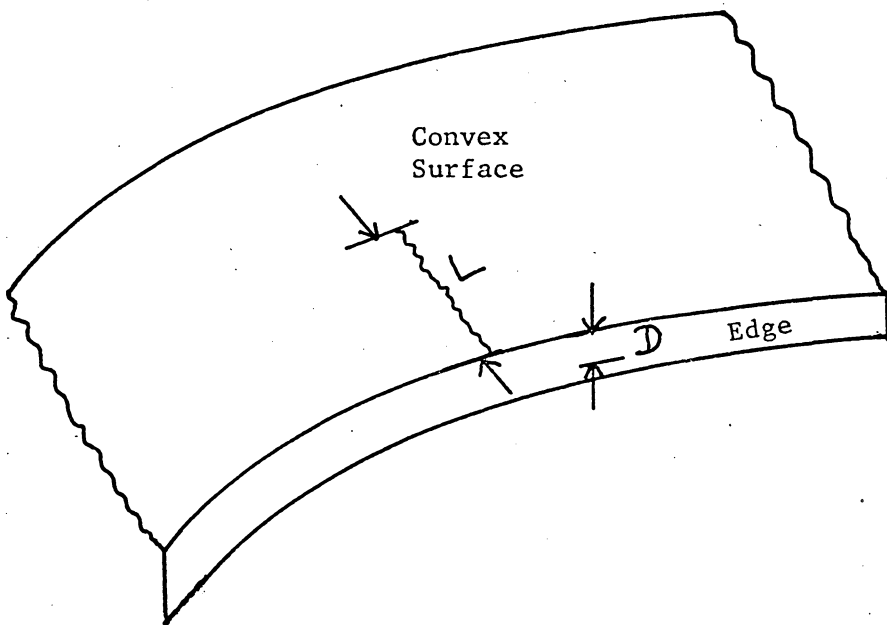


Figure 4. Schematic diagram of U-bend showing L and D.

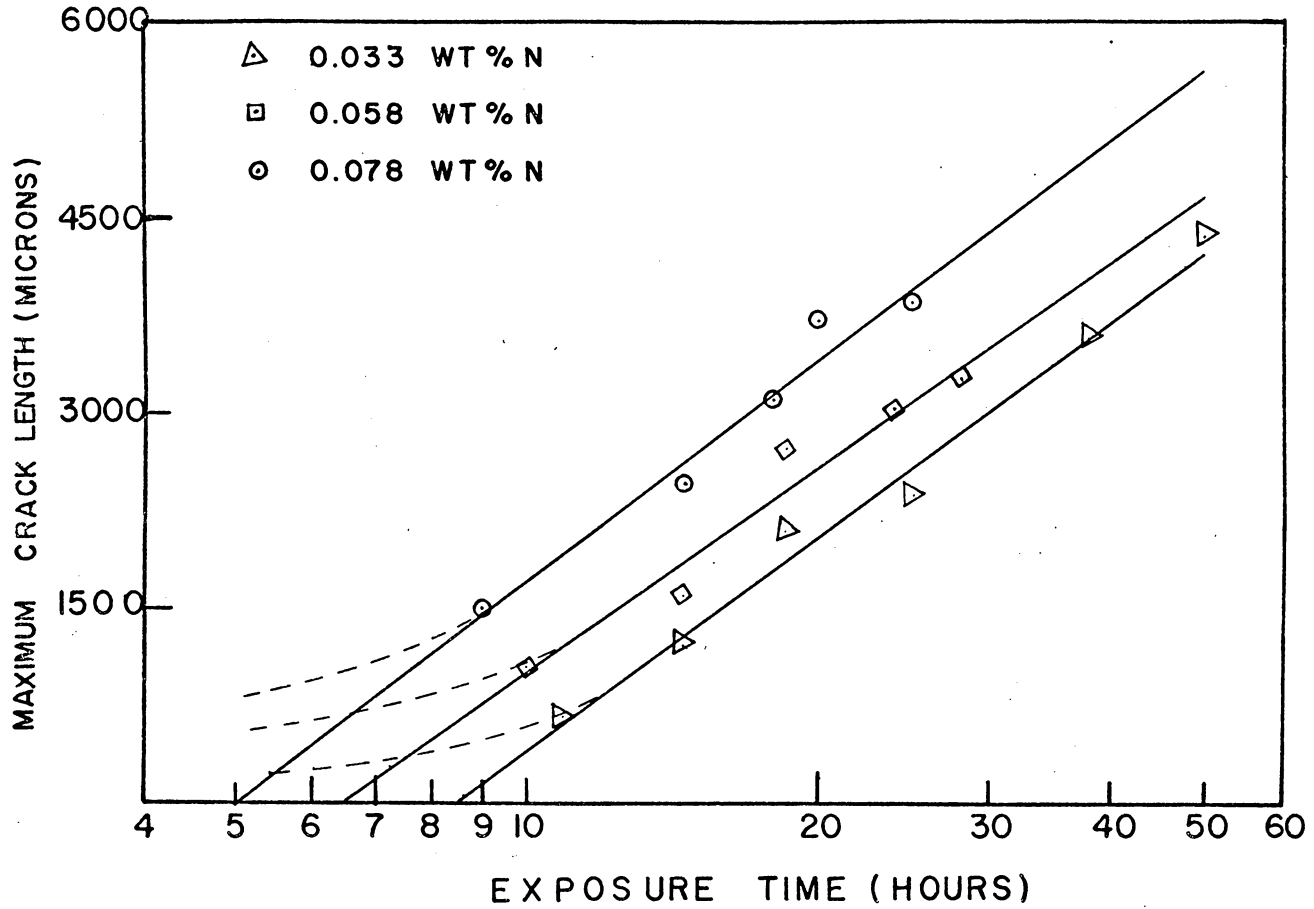


Figure 5. Relationship between maximum crack length L and exposure time t , for various nitrogen levels in type 310 stainless steel.

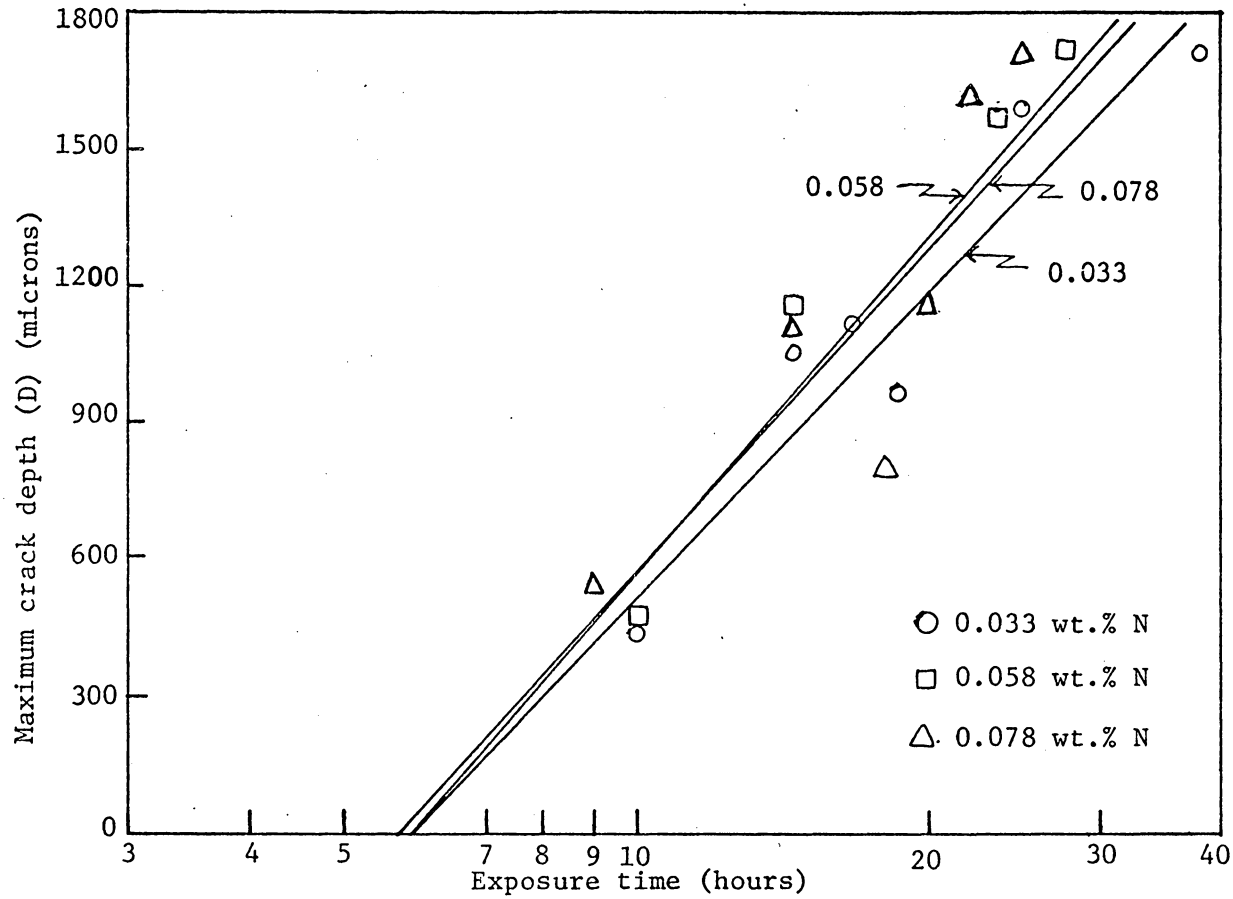


Figure 6. Relationship between maximum crack depth (D) and Exposure time t, for various nitrogen levels in type 310 stainless steel.

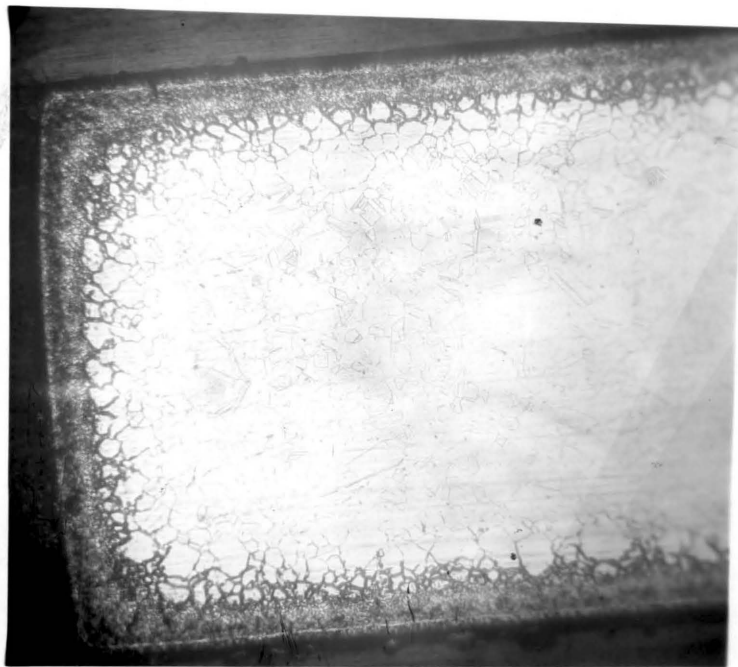


Figure 7a. Photomicrograph showing uniform nitrided case formed along the edges of a nitrided 20Cr-20Ni stainless steel specimen (0.161 wt.%). 50X.

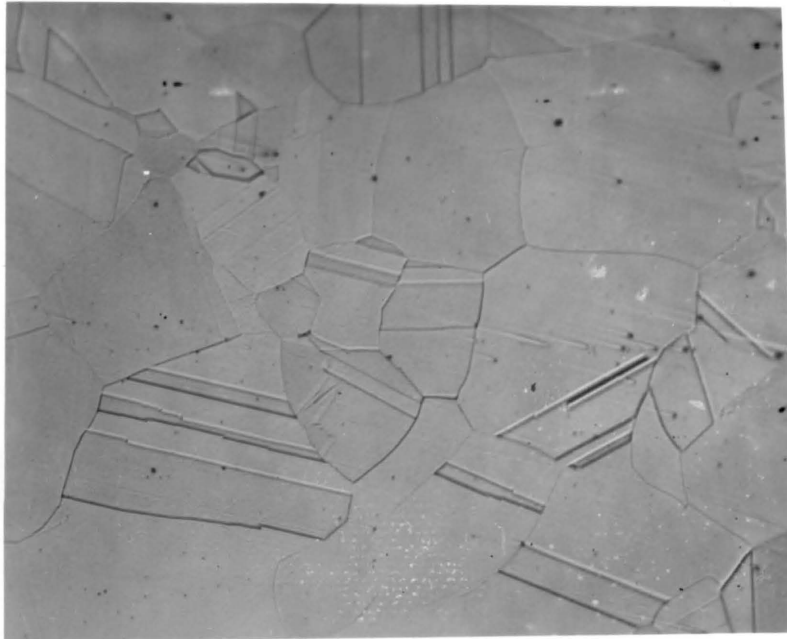


Figure 7b. As-homogenized microstructure of type 20Cr-20Ni stainless steel containing 0.161 wt.% nitrogen. 150X.

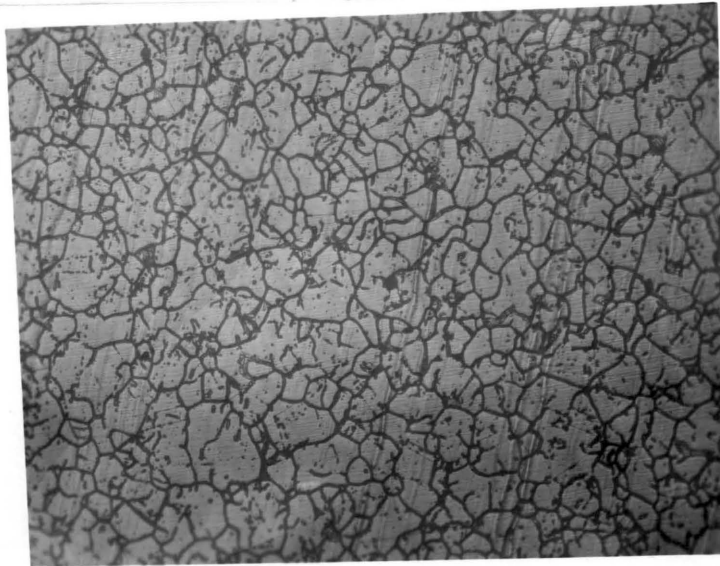


Figure 8a. As-nitrided microstructure of type 310 stainless steel containing 0.078 wt.% nitrogen. 150X.

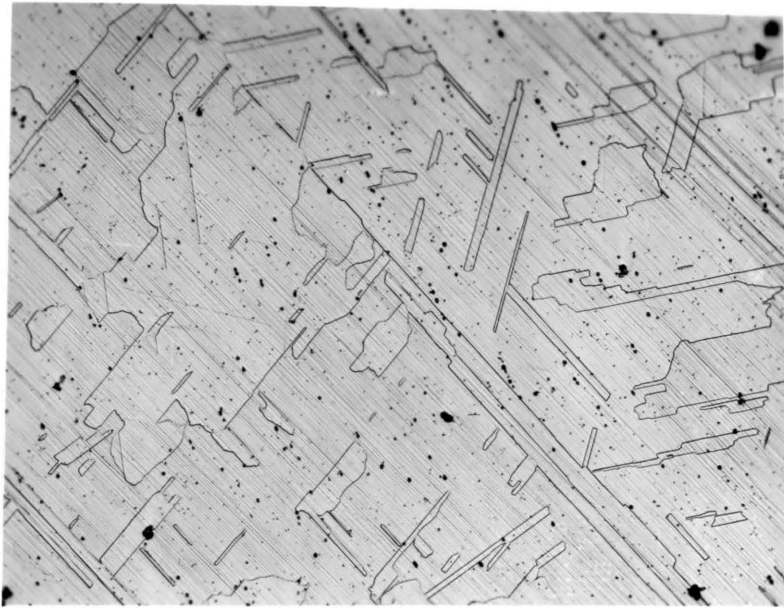


Figure 8b. As-homogenized microstructure of type 310 stainless steel containing 0.078 wt.% nitrogen. 150X.



Figure 9. Scanning electron micrograph showing transgranular nature of a stress-corrosion crack in type 310 stainless steel containing 0.058 wt.% nitrogen, tested for 18-1/2 hours in boiling magnesium chloride. 200X.

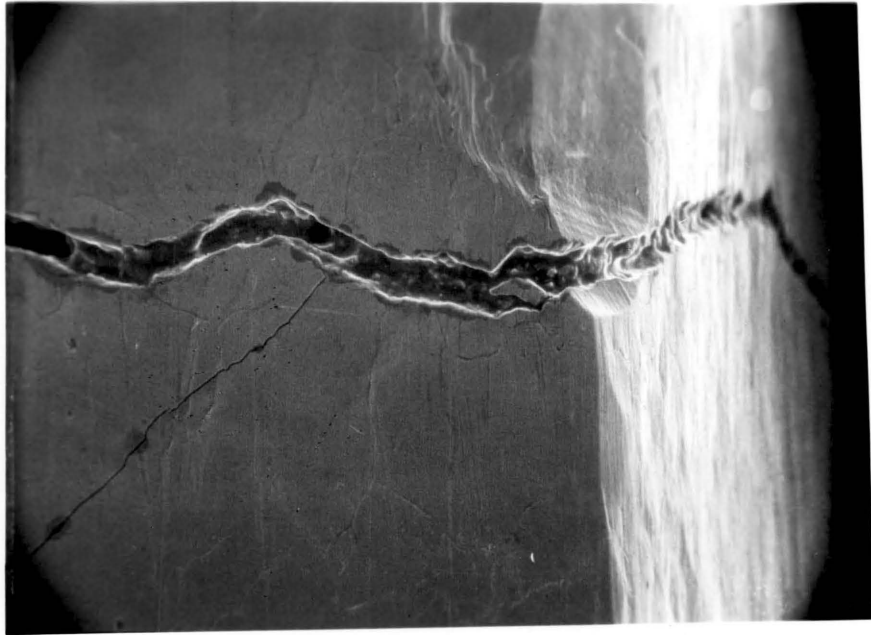


Figure 10. Example of a stress-corrosion crack observed in type 310 stainless steel U-bend specimen exposed for 18-1/2 hours in boiling MgCl_2 ; right side is the specimen outer edge, and convex face of the U-bend is at the left side. 200X.

TABLE I

Heat Analysis of type 20-20 High Purity Stainless Steel

<u>Element</u>	<u>Wt.%</u>
C	0.014
Mn	0.005
P	0.010
S	0.005
Si	0.035
Cr	19.5
Ni	19.8
N	0.004
O	0.007
Fe	Balance

TABLE II

Heat Analysis of type 310 Stainless Steel

<u>Element</u>	<u>Wt.%</u>
C	0.080
Mn	1.71
P	0.022
S	0.014
Si	0.50
Cu	0.17
Ni	19.7
Cr	24.5
Mo	0.27
N	0.033
Fe	Balance

TABLE III

Nitriding atmospheres and resulting nitrogen contents

<u>Alloy</u>	<u>Atmosphere</u>			<u>Temperature</u>	<u>Time</u>	<u>Wt.% N</u>
type 20Cr-20Ni	NH ₃	N ₂	H ₂			
	As Received					0.004
	60%	-	40%	1800°F	24 hrs.	0.161
type 310	As Received					0.033
	-	50%	50%	1100°F	24 hrs.	0.058
	-	50%	50%	1200°F	24 hrs.	0.078

TABLE IV

Solution annealing temperatures and times

<u>Type</u>	<u>Nitrogen Content</u>	<u>Annealing Temperature</u>	<u>Time</u>
20Cr-20Ni	0.004%	1950°F	24 hrs.
	0.161%	2300°F	30 mts.
310	0.033%	1950°F	24 hrs.
	0.058%	1950°F	24 hrs.
	0.078%	1950°F	24 hrs.

TABLE V

Relationship between exposure times and maximum crack length/depth for various nitrogen levels in type 310

<u>Alloy</u>	<u>Nitrogen Content</u> (wt.%)	<u>Exposure Time</u> (hours)	<u>Maximum Crack length/depth</u>	
			L (in micron)	D (in micron)
Type 20Cr-20Ni	0.004	50	no cracking	
		97		
		100		
		114		
		125		
		136		
		150		
		170		
		356		
	0.161	150	no cracking	
		260		
Type 310	0.033	11	651	465
		14-1/2	1236	1147
		18-1/2	2077	956
		25	2356	1586
		38	3509	1705
		50	4340	--
	0.058	10	1054	468
		14-1/2	1585	1149
		18-1/2	2725	1625
		24	3038	1563
		28	3255	1705
	0.078	9	1500	541
		14-1/2	2418	1123
		18	3100	806
		20	3720	1161
		25	3844	1601
		22	3800	1705

TABLE VI

Variation of rate of maximum crack propagation with penetration, for various nitrogen contents in type 310

<u>% N</u>	<u>% Penetration</u>	$\frac{dD}{dt} = \frac{0.4343M}{t}$		$\frac{dD}{dt} = \frac{D_m}{\tau_{Sc}} \exp(-t/\tau_{Sc})$	
		<u>using L</u>	<u>using D</u>	<u>using L</u>	<u>using D</u>
0.033	5	3.71	2.49	1.61	1.03
	10	2.64	2.28	1.56	1.00
	15	2.16	2.10	1.52	0.97
	20	1.64	1.92	1.44	0.94
	25	1.28	1.78	1.36	0.91
	30	0.99	1.62	1.27	0.87
0.058	5	4.61	3.63	1.95	1.34
	10	3.38	3.37	1.90	1.29
	15	2.58	3.07	1.82	1.22
	20	1.93	2.94	1.73	1.20
	25	1.47	2.67	1.63	1.30
	30	1.12	2.47	1.51	1.06
0.078	5	6.31	3.59	2.9	1.31
	10	4.61	3.33	2.79	1.27
	15	3.60	2.84	2.70	1.16
	20	2.88	2.82	2.57	1.14
	25	2.33	2.62	2.45	1.11
	30	1.81	2.38	2.17	1.05

VII. BIBLIOGRAPHY

1. Logan, H. L., The stress-corrosion of metals, John Wiley and Sons, Inc., New York, 1966.
2. Dixon, E. S., The book of stainless steel, ASM, 1935, p. 385.
3. Copson, H. R., Physical metallurgy of stress-corrosion fracture, interscience, New York, 1959.
4. Eckel, J. F., and Manning, Jr., C. R., A study of internal-friction peaks in type 304 stainless steel containing nitrogen, ASTM special publication No. 369.
5. Barnartt, S., and Van Rooyan, D., J. of Electrochemical Soc., 108, 1961, p. 222.
6. Uhlig, H. H., and White, R. A., Trans. ASM, 52, 1960, p. 830.
7. Lang, F. S., Corrosion, 18, 1962.
8. ASTM Special publication, 264, Philadelphia, Pa.
9. Snowden, P. P., J. of Iron and Steel Inst., 194, 1960.
10. Uhlig, H. H., Corrosion Handbook, John Wiley and Sons, Inc., New York, 1948, p. 569.
11. Harwood, J. J., Physical metallurgy of stress-corrosion fracture, interscience, New York, 1959, p. 19.
12. Forty, A. J. Physical metallurgy of stress-corrosion fracture, interscience, New York, 1959, p. 99.
13. Logan, H. L., Physical metallurgy of stress-corrosion fracture, interscience, New York, 1959, p. 143.
14. Hoar, T. P., and Hines, J. G., Stress-corrosion cracking and embrittlement, New York, 1956.
15. Clevinger, G. S., and Lytton, J. L., Virginia Polytechnic Institute and State University, Quarterly report No. 2, January 1971.
16. Keating, F. H., Symposium on stress-corrosion cracking, 1948, p. 329.

17. Nielson, N. A., Physical metallurgy of stress-corrosion fracture, Interscience, New York, 1959, p. 122.
18. Barnartt, S., Stickler, R., and Van Rooyan, D., Corrosion Science, 3, 1963, p. 9.
19. Van Rooyan, D., First international conference on metallic corrosion, Butterworth, London, 1961, p. 309.
20. Truman, J. E., and Perry, R., Brit. Corr. Jnl. 1, 1966, p. 60.
21. Ohtani, N., and Dodd, R. A., Corrosion, 21, 1965, p. 161.
22. Swann, P. R., Corrosion, 19, 1963, p. 102t.
23. Thomas, K. C., Stickler, R., and Allio, R. J., Corrosion Science, 5, 1965, p. 71.
24. Masamichi Kowaka and Hisao Fujikawa, The U. R. Evans international conference on localized corrosion, December 1971.
25. Robertson, W. D., and Tetleman, A. S., Strengthening mechanisms in solids, ASM, 1962, p. 217-252.
26. Uhlig, H. H., White, A., and Lincoln, Jr. Jr., Acta Met. 5, 1957, p. 473.
27. Uhlig, H. H., and Sava, J. P., Corrosion Science, 5, 1965, p. 291.
28. Ferry, B. N., Effect of nitrogen on AISI type 304 stainless steel non-equilibrium stress aging properties, M.S. Thesis, Virginia Polytechnic Institute, Blacksburg, Virginia, May 1966.
29. Cox, T. B., Some effects of nitrogen content on the stress-corrosion susceptibility of type 304 austenitic stainless steel, M.S. Thesis, Virginia Polytechnic Institute, Blacksburg, Virginia, April 1968.
30. Robertson, W. D., and Bakish, R., Acta. met. 3, 1955, p. 513.
31. Douglas, D. L., Thomas, G., and Roser, W. R., Corrosion, 1964, p. 15t.
32. Swann, P. R., and Nutting, J., Structure and properties of thin films, John Wiley and Sons, New York, 1959, p. 196.
33. Honeycomb, R. W. K., Paper presented at international conference, Relation of structure to mechanical properties, National physical laboratory, England, 1963.

34. Smith, R. E., The relationship of nitrogen to dislocation configurations in 20Cr-20Ni stainless steels deformed in tension, Ph.D. Dissertation, Materials Engineering Science, Virginia Polytechnic Institute, Blacksburg, Virginia, June 1968.
35. Clevinger, G. S., An electron microscopic study of the effects of aging on austenitic stainless steels containing nitrogen, M.S. Thesis, Virginia Polytechnic Institute, Blacksburg, Virginia, May 1968.
36. Maitra, S., Effects of nitrogen content on the susceptibility to stress-corrosion cracking of type 304 stainless steel wires, M.S. Thesis, Virginia Polytechnic Institute and State University, January 1972.
37. Eckel, J. F., and Cox, T. B., Bulletin of the Virginia Polytechnic Institute, Blacksburg, Virginia, January 1962.
38. Streicher, M. A., and Sweet, A. J., Corrosion, 25, January 1969, p. 1.
39. Eckel, J. F., Corrosion, 18, July 1962, p. 270t.
40. Dix, E. H., Trans. AIME, 137, 1940, p. 137.
41. Mears, R. B., Brown, R. H., and Dix, E. H., Symposium on stress-corrosion cracking of metals, ASTM-AIME, Philadelphia, 1945, p. 323.
42. Williams, W. L., Corrosion, 17, July 1961, p. 340t-344t.
43. Hines, J. G., Corrosion Science, 1, 1961, p. 21.
44. Logan, H. L., and Sherman, Jr., R. J., Welding Journal, 35, 1956, p. 389S.
45. Vaughan, D. A., Phalen, D. I., Peterson, C. L., and Boyd, W. K., Second international conference on metallic corrosion, March 11-15, 1963, New York, N. Y.

**The vita has been removed from
the scanned document**

THE EFFECT OF NITROGEN CONTENT ON THE
SUSCEPTIBILITY TO STRESS-CORROSION CRACKING
OF TYPE 20-Cr-20Ni AND AISI TYPE 310 STAINLESS STEELS

by

Ramaswamy Narayanan

(ABSTRACT)

The effect of nitrogen content on the susceptibilities of type 310 and 20Cr-20Ni stainless steels to stress-corrosion cracking were studied by exposing the U-bend specimens of the alloys containing various nitrogen levels to magnesium chloride solutions boiling at 154°C. It was found that the increase in nitrogen levels up to 0.161 wt.% did not induce cracking in type 20Cr-20Ni alloys even after long exposure times. At the same time, increase in nitrogen content decreased the crack initiation time in type 310 stainless steel and increased the depth of penetration. Furthermore, the rate of propagation of the stress-corrosion cracks in the U-bend stainless steel specimens of type 310 decreased with increase in exposure time.